

# Attitude Control of Satellite With Pulse-Width Pulse-Frequency (PWPF) Modulator Using Generalized Incremental Predictive Control

Ehsan Chegeni<sup>1</sup>, Mehdi Zandieh<sup>2</sup>, Javad Ebrahimi<sup>3</sup>

1- Young Researchers Club, Islamic Azad University, Boroujerd Branch, Boroujerd, Iran.

Email: ehsancheeni@hotmail.com

2- Department of Control Engineering, Islamic Azad University, Science and Research Boroujerd Branch, Boroujerd, Iran.

Email: zandieh.65@gmail.com

3- Young Researchers Club, Islamic Azad University, Boroujerd Branch, Boroujerd, Iran.

Email: jebrahimi@rocketmail.com

Received: July 2013

Revised: December 2013

Accepted: June 2014

## ABSTRACT:

In this paper, we use generalized incremental predictive control (GIPC) to stabilize attitude of satellite. We compare Generalized Predictive Control (GPC) with GIPC algorithm and present that GIPC has better performance. The three-axis attitude control systems are activated in pulse mode. Consequently, a modulation of the torque command is compelling in order to avoid high non-linear control action. This work considers the Pulse-Width Pulse-Frequency modulator (PWPF) is composed of a Schmitt trigger, a first order filter, and a feedback loop. PWPF modulator has several advantages over classical bang-bang controllers such as close to linear operation, high accuracy, and reduced propellant consumption.

**KEYWORDS:** Predictive Control; Satellite; GIPC; PWPF.

## 1. INTRODUCTION

The GPC method was proposed by Clarke et al. [1] and has become one of the most popular predictive control methods both in academia and industry. It can handle many different control problems for a wide range of plants with a reasonable number of design variables and constraints.

For improving performance of generalized predictive control, Generalized Incremental Predictive Control (GIPC) method is proposed by Ghahramani et al. [2], whose remove instabilities caused by actuator saturation. Further, it has a higher robustness with respect to the modeling uncertainties in comparison with GPC method.

The primary task of the control system is to stabilize the attitude of the satellite against external torque disturbances. Such disturbances are produced by aerodynamic drag effects, solar radiation and solar wind torques, parasitic torques created by the propulsion thrusters, and so on. Unfortunately, reaction controllers do not possess the same linear relationship between the input to the controller and its output torque. In fact, they are activated in an on-off mode. Nonetheless, they can be used in a quasi-linear mode by modulating the width of the activated reaction pulse proportionally to the level of the torque command input

to the controller. This is the often used Pulse Width modulation (PW) principle. A related design technique is based on the well-known Schmidt trigger, which implements a Pulse-Width Pulse-Frequency modulation (PWPF) in which the distance between the pulses is also modulated [4]. The basic goal is minimum time-fuel attitude control system to extend the life of a satellite.

This paper is organized as follows: In Section 2, Three degree of freedom satellite dynamics is modeled. In Section 3, MPC strategy and GIPC algorithm is presented. In Section 4,

PWPF modulator is explained. In Section 5, the results obtained from the simulation of GPC and GIPC methods for the satellite are given. Finally, Section 6 is devoted to conclusions.

## 2. THREE DEGREE OF FREEDOM SATELLITE DYNAMIC MODEL

Three degree of freedom (3-dof) rigid satellite model is presented in this section. Axes  $X_B$ ,  $Y_B$  and  $Z_B$  define the satellite's body axis frame, and the axis system is considered centered at the center of gravity (Fig. 1). Thrusters are available to produce torques about each of the three principal axes. The physical interpretation

of the Euler angles for a satellite platform is illustrated in Fig. 1. The roll ( $\phi$ ), pitch ( $\theta$ ) and yaw ( $\psi$ ) angles are defined by successive rotations around the coordinate axes  $X_B$ ,  $Y_B$  and  $Z_B$  in the body fixed frame. For large angles and position control of spacecraft, quaternion rotation is used. This is more suitable as it avoids singularity functions and gimbal lock [8].

Euler angular moment ( $\dot{H}$ ) which performs satellite attitude-rotational motion in space is expressed in the form of a matrix as follows:

$$\begin{aligned} M &= \frac{dH}{dt} + [\omega \times H] \\ \frac{dH}{dt} &= M - [\omega \times H], \quad H = I \cdot \omega \\ I \cdot \frac{d\omega}{dt} &= M - [\omega \times I \cdot \omega] \\ \frac{d\omega}{dt} &= \begin{bmatrix} \dot{p} \\ \dot{q} \\ \dot{r} \end{bmatrix} = I^{-1} \cdot M - [I^{-1} \cdot \omega] \times [I \cdot \omega] \end{aligned} \quad (1)$$

Where vector  $M$ , the applied moment (thrusters), is the input  $u$ , vector  $\omega$  is the angular rate and matrix  $I$  is the inertia around the body principal axes  $X_B, Y_B$  and  $Z_B$ . These are given as follow:

$$\begin{aligned} u &= [M_x \quad M_y \quad M_z]^T \\ \omega &= [p \quad q \quad r]^T \\ I &= \begin{bmatrix} I_{xx} & 0 & 0 \\ 0 & I_{yy} & 0 \\ 0 & 0 & I_{zz} \end{bmatrix} \end{aligned} \quad (2)$$

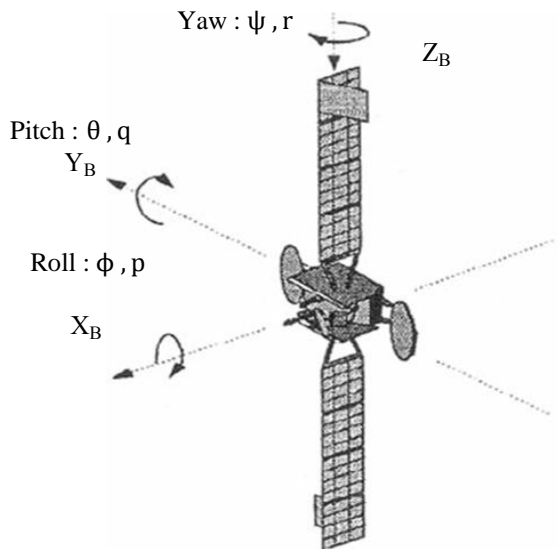


Fig. 1. Satellite reference and body coordinates. Solving (1) and (2)

$$\begin{bmatrix} \dot{p} \\ \dot{q} \\ \dot{r} \end{bmatrix} = \begin{bmatrix} \frac{M_x - q \cdot I_{zz} \cdot r + r \cdot I_{yy} \cdot q}{I_{xx}} \\ \frac{M_y - r \cdot I_{xx} \cdot p + p \cdot I_{zz} \cdot r}{I_{yy}} \\ \frac{M_z - p \cdot I_{yy} \cdot q + q \cdot I_{xx} \cdot p}{I_{zz}} \end{bmatrix} \quad (3)$$

The relationship between body rate  $\omega_b = [p_b \quad q_b \quad r_b]^T$  of the satellite and angular rates  $\omega = [\dot{\phi} \quad \dot{\theta} \quad \dot{\psi}]^T$  is defined by the following transformation:

$$\begin{aligned} \begin{bmatrix} \dot{\phi} \\ \dot{\theta} \\ \dot{\psi} \end{bmatrix} &= \begin{bmatrix} 1 & \frac{\sin(\phi)\sin(\theta)}{\cos(\theta)} & \frac{\sin(\phi)\sin(\theta)}{\cos(\theta)} \\ 0 & \cos(\phi) & -\sin(\phi) \\ 0 & \frac{\sin(\phi)}{\cos(\theta)} & \frac{\cos(\phi)}{\cos(\theta)} \end{bmatrix} \begin{bmatrix} p \\ q \\ r \end{bmatrix} \\ \Rightarrow \begin{bmatrix} \dot{\phi} \\ \dot{\theta} \\ \dot{\psi} \end{bmatrix} &= \begin{bmatrix} p + \frac{(q\sin(\phi) + r\cos(\phi))\sin(\theta)}{\cos(\theta)} \\ q\cos(\phi) - r\sin(\phi) \\ \frac{q\sin(\phi) + r\cos(\phi)}{\cos(\theta)} \end{bmatrix} \end{aligned} \quad (4)$$

The non-linear state model of the satellite can be derived by partial derivatives of the model states  $x = [p_b, q_b, r_b, \phi_I, \theta_I, \psi_I]^T$

$$\begin{bmatrix} \dot{p}_b \\ \dot{q}_b \\ \dot{r}_b \\ \dot{\phi}_I \\ \dot{\theta}_I \\ \dot{\psi}_I \end{bmatrix} = \begin{bmatrix} \frac{M_x - q \cdot I_{zz} \cdot r + r \cdot I_{yy} \cdot q}{I_{xx}} \\ \frac{M_y - r \cdot I_{xx} \cdot p + p \cdot I_{zz} \cdot r}{I_{yy}} \\ \frac{M_z - p \cdot I_{yy} \cdot q + q \cdot I_{xx} \cdot p}{I_{zz}} \\ p + \frac{(q\sin(\phi) + r\cos(\phi))\sin(\theta)}{\cos(\theta)} \\ q\cos(\phi) - r\sin(\phi) \\ \frac{q\sin(\phi) + r\cos(\phi)}{\cos(\theta)} \end{bmatrix} \quad (5)$$

**Table 1. Satellite Parameters**

Parameters	Description	Value
$I_{xx}$	Moment of inertia (x-axis)	1.928 kgm <sup>2</sup>
$I_{yy}$	Moment of inertia (y-axis)	1.928 kgm <sup>2</sup>
$I_{zz}$	Moment of inertia (z-axis)	4.953 kgm <sup>2</sup>
Thruster	Input to satellite (Mx , My , Mz)	1 kgm <sup>2</sup>
$\phi_0$	Initial roll Euler angle	0.362 rad
$\theta_0$	Initial pitch Euler angle	0.524 rad
$\psi_0$	Initial yaw Euler angle	-0.262 rad
p	Body pitch roll rate	0 rad/s
q	Body yaw rate	0 rad/s
r	Body roll rate	0 rad/s

$A=Jacobian(f(x),x)$  ,  $B=Jacobian(f(x),u)$

$$A = \begin{bmatrix} 0 & \frac{-rI_{zz} + rI_{yy}}{I_{xx}} & \frac{-qI_{zz} + qI_{yy}}{I_{xx}} & 0 \\ \frac{-rI_{xx} + rI_{zz}}{I_{yy}} & 0 & \frac{-pI_{xx} + pI_{zz}}{I_{yy}} & 0 \\ \frac{-qI_{yy} + qI_{xx}}{I_{zz}} & \frac{-pI_{yy} + pI_{xx}}{I_{zz}} & 0 & 0 \\ 1 & \frac{\sin\phi(\sin\theta)}{\cos\theta} & \frac{\cos\phi(\sin\theta)}{\cos\theta} & \frac{q\cos\phi - r\sin\phi(\sin\theta)}{\cos^2\theta} \\ 0 & \cos\phi & -\sin\phi & -q\sin\phi - r\cos\phi \\ 0 & \frac{\sin\phi}{\cos\theta} & \frac{\cos\phi}{\cos\theta} & \frac{-q\cos\phi - r\sin\phi}{\cos\theta} \end{bmatrix}$$

$$B = \begin{bmatrix} 0 \\ 0 \\ 0 \\ q\sin\phi + r\cos\phi + \frac{(q\sin\phi + r\cos\phi)(\sin^2\theta)}{\cos^2\theta} \\ 0 \\ 0 \\ q\sin\phi + \frac{r\cos\phi(\sin\theta)}{\cos^2\theta} \\ 0 \end{bmatrix}$$

$$B = \begin{bmatrix} \frac{1}{I_{xx}} & 0 & 0 & 0 & 0 & 0 \\ 0 & \frac{1}{I_{yy}} & 0 & 0 & 0 & 0 \\ 0 & 0 & \frac{1}{I_{zz}} & 0 & 0 & 0 \\ 0 & 0 & 0 & 0 & 0 & 0 \\ 0 & 0 & 0 & 0 & 0 & 0 \\ 0 & 0 & 0 & 0 & 0 & 0 \end{bmatrix} \quad (6)$$

Where matrix  $A(x)$  and  $B(u)$  are Jacobian matrix of non-linear function  $f(x)$  with respect to state vector  $x = [p, q, r, \phi, \theta, \psi]^T$  and input vector  $u = [M_x, M_y, M_z, 0, 0, 0]^T$ , respectively. The satellite parameters in Table 1 are given in [3].

**3. MODEL PREDICTIVE CONTROL AND GIPC ALGORITHM**

The success of the methods based on model based predictive control is their ability to explicitly handle constraints, processes with delays, and nonlinear systems [5]. As shown in Fig. 2, model uses past inputs and outputs of system to predict  $N_y$  step future outputs.  $N_y$  is called prediction horizon. Vector of future optimal control signals obtain by measuring prediction error and minimizing cost function.

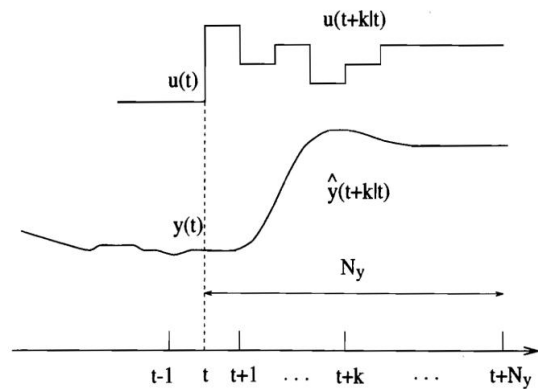


**Fig. 2. MPC strategy**

$$\Delta U = [\Delta u(t|t) \quad \Delta u(t+1|t) \quad \dots \quad \Delta u(t+N_u-1|t)]^T \quad (7)$$

Where  $N_u$  is called control horizon and equals to length of obtained vector from optimization problem. Therefore, first control signal  $\Delta u(t|t)$  is applied to system and next signals are rejected. At the next sampling instant, prior step is repeated with this new value and all the sequences are brought up to date. Thus the  $\Delta u(t+1|t+1)$  is calculated (which in principle will be different to the  $\Delta u(t+1|t)$  because of the new information available) using the receding horizon concept [1].

**3.1. GIPC algorithm**

In state-space modeling of the standard MPC, the present states are used to predict the states. But, in the new receding-horizon algorithm named Generalized Incremental Predictive Control, both present and previous states rather than present states are considered in the  $j$  step ahead prediction of the states and outputs.

Therefore, the optimal solution includes the weighted difference of the current and the previous states and the summation of the control action increments. Using the weighted difference of the states in control action provides a faster response and improves the robustness of the system [2]. Consider the following state-space model:

$$\begin{cases} x(k+1) = Ax(k) + Bu(k) \\ y(k+1) = Cx(k+1) \end{cases} \quad (8)$$

$x \in R^n$ ,  $u \in R$  and  $y \in R$  denote the state vector, system input, and system output, respectively. Also matrices  $A \in R^{n \times n}$ ,  $B \in R^n$ , and  $C \in R^n$  are system matrices. The incremental form of the state predictions is given by:

$$\Delta x(k+1) = A\Delta x(k) + B\Delta u(k) \quad (9)$$

Where

$$\begin{aligned} \Delta u(k) &= u(k) - u(k-1), \Delta x(k) = x(k) - x(k-1) \\ \Delta x(k+1) &= x(k+1) - x(k) \end{aligned} \quad (10)$$

By combining (9), (10) gives:

$$x(k+1) = (A+I)x(k) - Ax(k-1) + B\Delta u(k) \quad (11)$$

Where  $I$  is the identity matrix. This equation describes the one-ahead prediction of states in terms of the current states  $x(k)$  and the previous states  $x(k-1)$ . Finally, the general form of  $j$  step-ahead predictions of the states is given by:

$$\begin{aligned} x(k+j) &= \left( \sum_{m=0}^j A^m \right) x(k) - \left( \sum_{m=1}^j A^m \right) x(k-1) \\ &+ \sum_{n=1}^j \left( \sum_{m=0}^{n-1} A^m \right) B\Delta u(k+j-n) \end{aligned} \quad (12)$$

From Eq. (12), outputs prediction over the prediction horizon  $N_y$  and the control horizon  $N_u$  can be written as the following compact matrix/vector form:

$$Y = P_{y0}x(k) - P_{y1}x(k-1) + H_y\Delta U \quad (13)$$

Where

$$\begin{aligned} Y &= \begin{bmatrix} y(k+1) \\ y(k+2) \\ \vdots \\ y(k+N_y) \end{bmatrix}, \Delta U = \begin{bmatrix} \Delta u(k) \\ \Delta u(k+1) \\ \vdots \\ \Delta u(k+N_u-1) \end{bmatrix}, \\ P_{y0} &= \begin{bmatrix} C(A+I) \\ C(A^2+A+I) \\ \vdots \\ C\left(\sum_{i=0}^{N_y} A^i\right) \end{bmatrix} \\ P_{y1} &= \begin{bmatrix} CA \\ C(A^2+A) \\ \vdots \\ C\left(\sum_{i=1}^{N_y} A^i\right) \end{bmatrix}, \\ H_y &= \begin{bmatrix} CB & 0 & \dots & 0 \\ C(A+I)B & CB & \dots & 0 \\ \vdots & \vdots & \ddots & \vdots \\ C\left(\sum_{i=0}^{N_y-1} A^i\right)B & C\left(\sum_{i=0}^{N_y-2} A^i\right)B & \dots & CB \end{bmatrix} \quad (14) \end{aligned}$$

Now, consider following cost function

$$J = (W - Y)^T Q (W - Y) + \Delta U^T \Delta U \quad (15)$$

Where

$$W = [w(k+1) \quad w(k+2) \quad \dots \quad w(k+N_y)]^T$$

is the reference trajectory.  $Q$  and  $R$  are positive definite and the weight of error and control signals respectively.

By posing eq. (13) in cost function eq. (15) and derivative toward  $\Delta U$  and equals it to zero, the optimal control vector is obtained as follows: [2]

$$\begin{aligned} \Delta U &= \left( H_y^T Q H_y + R \right)^{-1} H_y^T Q \\ &\left( W - P_{y0}x(k) + P_{y1}x(k-1) \right) \end{aligned} \quad (16)$$

**4. PWPF MODULATOR**

Pulse thruster devices can provide only on-off signals generating nonlinear control action. Nonetheless, those can be used in a quasi-linear mode by modulating the width of the activate reaction pulse proportionally to the level of the torque command input. This is known as pulse-width modulation (PW). In the pulse-width pulse-frequency (PWPF) modulation the distance between the pulses is also modulated. Its basic structure is shown in Fig. 3.

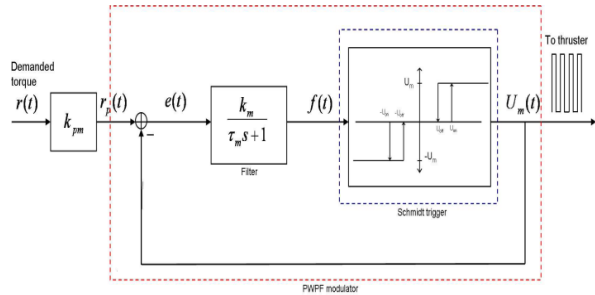


**Fig. 3.** PWPF modulator

The modulator includes a Schmitt trigger which is a relay with dead zone and hysteresis, it includes also a first-order-filter, lag network type, and a negative feedback loop. When a positive input to the Schmitt trigger is greater than  $U_{on}$ , the trigger output is  $U_m$ . If the input falls below  $U_{off}$  the trigger output is 0. This response is also reflected for negative inputs in case of two side-thrusters or those thruster that produce negative torques (clockwise direction). The error signal  $e(t)$  is the difference between the Schmitt trigger output  $U_{on}$  and the system input  $r(t)$ . The error is fed into the filter which output signal  $f(t)$  and it feeds the Schmitt trigger. For designing PWPF, consider these parameters:

- The filter coefficients  $K_m$  and  $\tau_m$ .
- The Schmitt trigger parameters  $U_{on}$ ,  $U_{off}$ , it defines the hysteresis as  $h=U_{on} - U_{off}$ .
- The maximal/minimal  $\pm U_m$ .

The PWPF modulator can incorporate an additional gain  $K_{pm}$  which will be considered separately from the control gain. In the case of a constant input, the PWPF modulator drives the thruster valve with on-off pulse sequence having a nearly linear duty cycle with input amplitude [6, 7].

**Table 2.** Recommended value for the PWPF parameters

$K_m$	$\tau_m$	$U_{on}$	H	$K_{pm}$
1	0.1	0.45	0.3	50

**5. NUMERICAL SIMULATION**

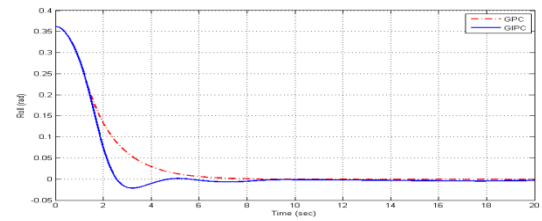
In this section, GPC and GIPC algorithm are applied to three degree of freedom satellite and are being

compared both algorithms. These simulations are implemented with table 3 values.

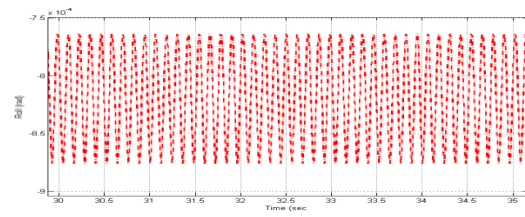
**Table 3.** Recommended value for the PWPF parameters

Q	R	$N_u$	$N_y$
7.I	1.I	3	200

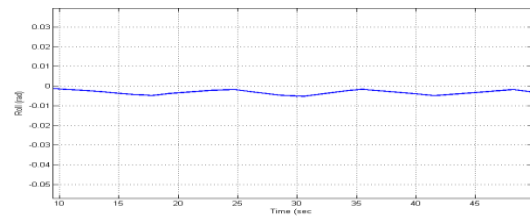
Fig. 4, Fig. 5 and Fig. 6 are presented Euler angles  $\phi, \psi, \theta$  under GPC and GIPC control. As seen in Fig. 4-a, Fig. 5-a and Fig. 6-a, it seems that GPC has faster response than GIPC, but according to more accurate Fig. 4-b,c, Fig. 5-b,c, Fig. 6-b,c, we find that the angles under GPC control with PWPF modulator have higher frequency fluctuations and more severe nonlinear operation toward GIPC. In fact, GIPC has pseudo-linear (nearly linear) operation.



a. Roll angle

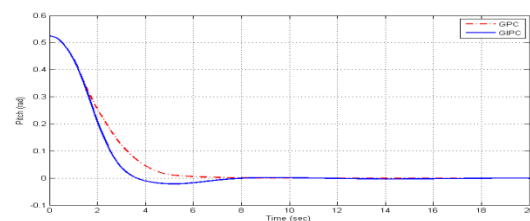


b. More accurate under GPC method

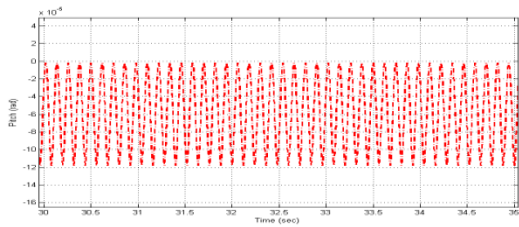


c. More accurate under GIPC method

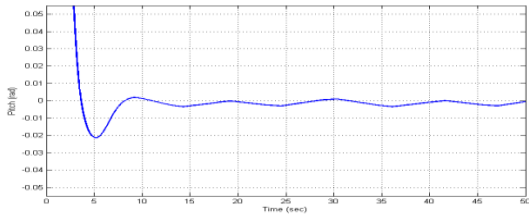
**Fig. 4.**



a. Pitch angle

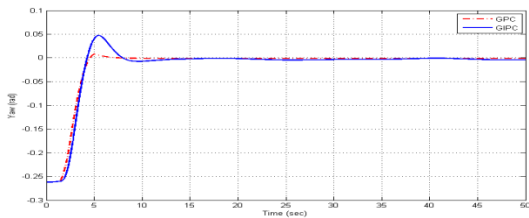


b. More accurate under GPC method

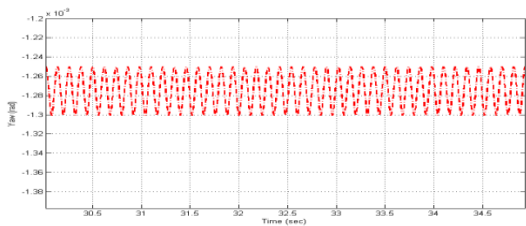


c. More accurate under GPC method

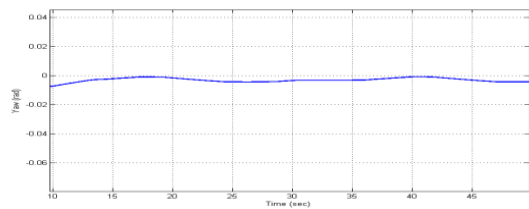
**Fig. 5.**



a. Yaw angle



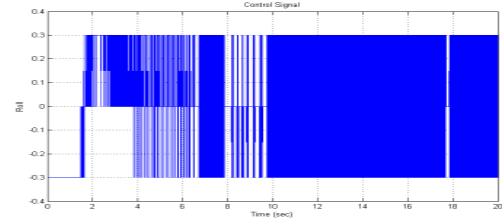
b. More accurate under GPC method



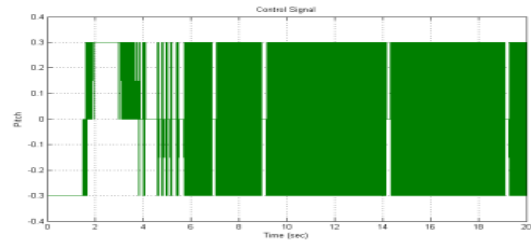
c. More accurate under GPC method

**Fig.6.**

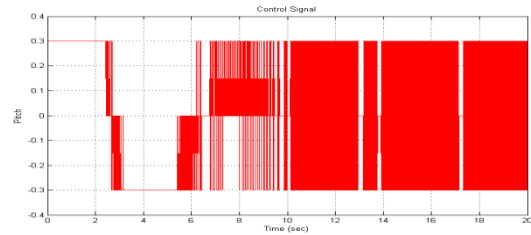
Modulated control signals are shown in Fig 7. Modulator present small pulse-width modulation which leads small impulses and hence less fuel consumption.



a. Roll control signal and PWWF modulation



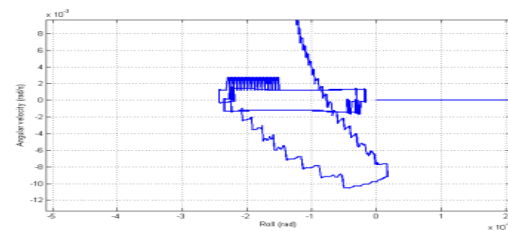
b. Pitch control signal and PWWF modulation



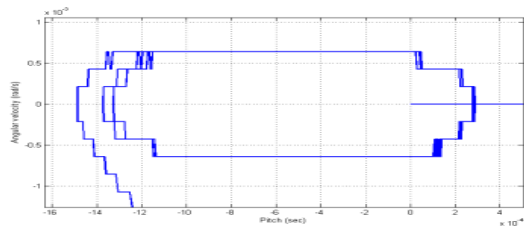
c. Yaw control signal and PWWF modulation

**Fig. 7.** Control signals and PWWF modulation

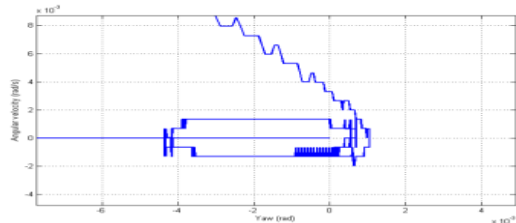
Another aspect of PWWF modulated systems is that they will be subject to self sustained oscillations because of the nonlinearities in the system. These oscillations are called limit cycles. In this satellite system, the limit cycles occur because of the minimum thruster on-time. In the simulations, the limit cycling will appear as a oscillation around the steady state. The duty cycle generated by the PWWF modulation is shown in Fig. 8. The specification of pointing accuracy is achieved, less than 0.01 degrees. It shows a high accurate performance of the reaction thruster which is possible by modulating the control signal using the PWWF modulator.



a. Roll limit cycle



b. Pitch limit cycle behavior about the steady state point in phase plane



c. Yaw limit cycle behavior about the steady state point in phase plane

**Fig .8.** Limit cycles behavior about the steady state point in phase plane

## 6. CONCLUSIONS

As it was observed, satellite system under GIPC method has better performance and more stability operation than GPC. The obtained results demonstrate the feasibility of combining GIPC/PWPF modulator in a unique controller for on-off thruster reaction attitude control system. Stability remains by adding the PWPF modulator and reasonable accuracy in attitude is achieved. GIPC method considers the present states as well as the previous states. Consequently, the resulting controller GIPC includes the weighted difference of the current and the previous states and the summation of the control action increments. Meanwhile, magnitude of the limit cycle has reduced i.e. response of system under GIPC/PWPF has extremely Low steady-state error.

It should be noted that GIPC controller can be made to eliminate disturbance because of the integrator and that is why the limit cycle oscillation frequency is less.

## REFERENCES

- [1] J.M., Maciejowski, “**Predictive Control with constraints**”, *Prentice Hall*, London, 2002.
- [2] N.O., Ghahramani , F., Towhidkhah, “**Constrained incremental predictive controller design for a flexible joint robot**”, *ISA Transactions* 48, pp. 321-326, 2009.
- [3] F., Nagi, S.K., Ahmed, A.A., ZainulAbidin, F.H.Nordin, “**Fuzzy bang-bang relay controller for satellite attitude control system**”, *Fuzzy Sets and Systems*, Elsevier, pp. 3-5, 2009.
- [4] S.J., Marcel, “**Spacecraft Dynamics and Control—A Practical Engineering Approach**”, *Cambridge University Press*, New York, 1997.

- [5] E.F., Camacho , C., Bordons, “**Model Predictive Control**”, *Springer*, Berlin, 1998.
- [6] G., Arantes Jr.,L.S., Martins-Filho and A.C., Santana,“**Optimal On-Off Attitude Control for the Brazilian Multimission Platform Satellite**”, *Mathematical Problems in Engineering*,pp.8-9,2009.
- [7] T. D. Krovel, “**Optimal Tuning of PWPF Modulator for Attitude Control**”, *Master Thesis, Department of Engineering Cybernetics, Norwegian University of Science and Technology*, pp12-17, 2005.
- [8] J.Y., Hung, W., Gao and J.C., Hung, “**Variable structure control: a survey**”, *IEEE Transactions on Industrial Electronics* 40 (1) (1993) 2–21.